

## Phenomenological Model of Diffraction and Resonant Scattering

T. LASINSKI AND R. LEVI SETTI

*The Enrico Fermi Institute for Nuclear Studies and Department of Physics,  
The University of Chicago, Chicago, Illinois\**

AND

E. PREDAZZI†

*Istituto di Fisica dell'Università di Torino, Torino, Italy  
and*

*Istituto Nazionale di Fisica Nucleare-Sezione di Torino, Torino, Italy*

(Received 5 July 1967)

Diffraction phenomena are shown to play an important role in  $K^-p \rightarrow K^-p$  elastic scattering, even in the region of  $\sim 1$  GeV/c, where resonant effects are dominant. A brief review of existing data indicates that the differential cross sections consistently exhibit an exponential behavior at small momentum transfers from  $\sim 16$  down to  $\sim 0.8$  GeV/c, and that the scattering amplitudes throughout this region are predominantly imaginary. The slope of the diffractionlike peak is shown to increase sharply at incident  $K^-$  momenta, corresponding to the formation of known, highly elastic resonances. A model is then formulated to apply to  $(\pi, K)$ -nucleon two-body processes, in which the scattering amplitudes for each isospin state are described by a linear superposition of diffractive and resonant contributions. On a purely empirical basis, the diffractive amplitudes have been parametrized in terms of an exponential  $t$  dependence. The model has been specialized to interpret  $K^-p \rightarrow K^-p$  elastic-scattering data from 0.8 to 1.2 GeV/c, where two dominant resonant states are known, the  $Y_1^*(1760)$  and  $Y_0^*(1820)$ . A good fit to the data yields a reliable set of six resonant parameters (masses, widths, and elasticities) for these states, and three parameters describing the diffractive contribution (real and imaginary part of the forward-scattering amplitude, and slope of the diffraction peak).

### 1. INTRODUCTION

IN recent years much evidence has been accumulated showing that diffraction phenomena, while dominating the high-energy behavior of elastic-scattering processes, may give important contributions even in the energy region which is usually considered to be the domain of resonant state formation.

Two of the present authors<sup>1</sup> and Gelfand *et al.*<sup>2</sup> have shown, in fact, that for  $K^-p \rightarrow K^-p$ , diffraction effects are felt even in the region of  $K^-$  laboratory momenta of about 1 GeV/c, where two prominent resonant states, the  $Y_1^*(1760)$  and  $Y_0^*(1820)$ , are formed. Similarly, diffractionlike peaks in the forward scattering  $\pi^\pm p \rightarrow \pi^\pm p$  have been pointed out by several authors (see, e.g., Damouth *et al.*<sup>3</sup>) above 1-GeV/c  $\pi$  laboratory momentum, in a region where many  $N^*$  states are known.

In Ref. 1, a simple model which assumes a predominantly imaginary diffractive scattering amplitude as a background, together with two resonant amplitudes, was shown to account for the  $K^-p \rightarrow K^-p$  data of

Gelfand *et al.*<sup>2</sup> in the momentum region 0.8–1.2 GeV/c.

In this paper we review first some of the evidence which has led to the formulation of the phenomenological model proposed here (Sec. 2). In Sec. 3 we define the scattering amplitudes on which the model is based for  $K^\pm p$  and  $\pi^\pm p$  elastic and charge-exchange scattering. In particular, each isospin amplitude will be described as a sum of a diffractive term having an exponential  $t$  dependence ( $t$  is the momentum transfer squared) and of an arbitrary number of resonant terms, each parametrized by their Breit-Wigner behavior. From these amplitudes, the differential cross sections and the polarizations are calculated as well as expressions for the coefficients of their Legendre series expansion. Relevant computational details are contained in Appendix A. In Sec. 4 we describe, as an example, a fit of our model to the experimental  $K^-p \rightarrow K^-p$  data of Gelfand *et al.*,<sup>2</sup> where only two resonant terms have so far been retained. Some concluding remarks and the relevance of this approach to the fit of a wider range of similar experimental data are discussed in Sec. 5.

### 2. EXPERIMENTAL EVIDENCE AND PARAMETRIZATION OF DIFFRACTION SCATTERING IN THE RESONANCE REGION

We limit ourselves here to a detailed consideration of the elastic scattering  $K^-p \rightarrow K^-p$  data, whose features in the 1-GeV/c region have motivated this study.

In the region of a few GeV/c up to the highest momenta available to date ( $\sim 16$  GeV/c), several

\* Research sponsored in part by the Air Force Office of Scientific Research, Office of Aerospace Research, U. S. Air Force, under AFOSR Contract No. AF 49(638)-1652 and by the National Science Foundation.

† Work supported in part by U. S. Air Force Grant EOAR No. 66-29.

<sup>1</sup> R. Levi Setti and E. Predazzi, in *Proceedings of the Thirteenth International Conference on High-Energy Physics, Berkeley, California, 1966* (University of California Press, Berkeley, 1967).

<sup>2</sup> N. M. Gelfand, D. Harmsen, R. Levi Setti, E. Predazzi, M. Raymond, J. Doede, and W. Männer, *Phys. Rev. Letters* **17**, 1224 (1966).

<sup>3</sup> D. E. Damouth, L. W. Jones, and M. L. Perl, *Phys. Rev. Letters* **11**, 287 (1963).

authors have obtained good fits to the  $K^-p \rightarrow K^-p$  forward-scattering data by using various optical models<sup>4-8</sup> (e.g., diffractive disk, annulus, absorptive gaussian potentials, etc.), as well as models based on the dominance of Regge poles (see, e.g., Ref. 9). Even in the energy region 0.78–1.22 GeV/c studied experimentally by Gelfand *et al.*,<sup>2</sup> effects which may be attributed to diffraction scattering can be detected by the presence of a pronounced forward peak in the  $K^-p \rightarrow K^-p$  differential cross sections. These cross sections, which will be discussed in more detail in Sec. 4, are reproduced in Fig. 1. In all cases the forward peak is consistent with an exponential behavior over the interval  $0 < -t \lesssim 0.4$  (GeV/c)<sup>2</sup>.

Independent evidence of diffractive phenomena can be derived from a comparison of the measured differential cross sections at  $0^\circ$ ,  $(d\sigma/d\Omega)_{\theta=0^\circ}$ , with the values obtained from the total cross sections by making use of the optical theorem.

As can be seen from the relation

$$\left(\frac{d\sigma}{d\Omega}\right)_{\theta=0^\circ} = |f(k,0)|^2 \geq [\text{Im}f(k,0)]^2 = \frac{k^2\sigma_{\text{tot}}^2}{(4\pi)^2} \equiv \left(\frac{d\sigma}{d\Omega}\right)_{\text{opt}} \quad (1)$$

where  $f(k,0)$  is the scattering amplitude at  $0^\circ$  for the center-of-mass (c.m.) momentum  $k$ , the equality sign in Eq. (1) implies a pure imaginary forward-scattering amplitude, a situation which is characteristic of diffraction scattering.

Indeed, it has been pointed out by several authors that above  $\sim 3$  GeV/c the  $K^-p \rightarrow K^-p$  forward-scattering amplitude is predominantly imaginary. In fact, the ratio of the real to the imaginary parts of the scattering amplitude, as obtained from the comparison between  $(d\sigma/d\Omega)_{0^\circ}$  and  $(d\sigma/d\Omega)_{\text{opt}}$ , was found not to exceed  $\sim 20\%$  at momenta of 4.5 and 5.5 GeV/c<sup>10</sup> and was indistinguishable from zero at  $\sim 10$  GeV/c.<sup>11</sup>

Gelfand *et al.*<sup>12</sup> have reported a comparison of their

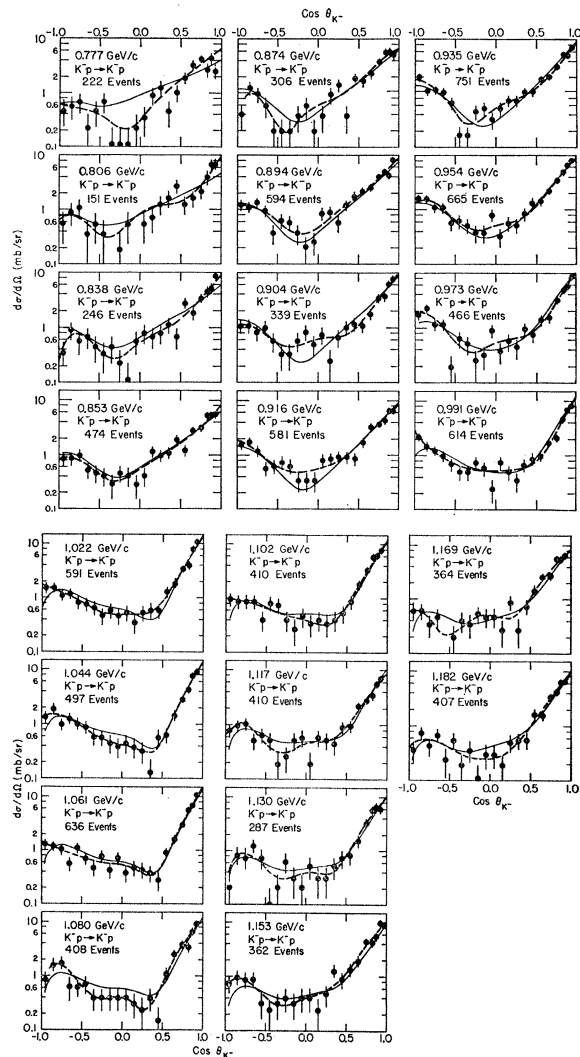


FIG. 1.  $K^-p \rightarrow K^-p$  differential cross sections from 0.777 to 1.183 GeV/c of Gelfand *et al.* (Ref. 2). The broken-line curves represent fits to the data in terms of sixth-order Legendre polynomial series expansions. The full-line curves correspond to the predictions of the model described in the paper, for the parameters obtained from the best fit to the Legendre coefficients  $A_0$ – $A_5$  (solution A). It should be noted that the fit was made in the region 0.874–1.130 GeV/c.

extrapolated forward differential cross sections between 0.8 and 1.2 GeV/c with the optical points obtained from a collection of total-cross-section data. This comparison is reproduced in Fig. 2 (the total-cross-section data here have been taken from Refs. 13 and 14) and leads to the speculation that, aside from deviations which will be shown to be due to resonant effects, even

<sup>4</sup> V. Cook, B. Cork, T. F. Hoang, D. Keefe, L. T. Kerth, W. A. Wenzel, and T. F. Zipf, Phys. Rev. **123**, 320 (1961).

<sup>5</sup> R. Crittenden, H. J. Martin, W. Kernan, L. Leipuner, A. C. Li, F. Ayer, L. Marshall, and M. L. Stevenson, Phys. Rev. Letters **12**, 429 (1964); L. Marshall and T. Oliphant, Phys. Letters **18**, 83 (1965).

<sup>6</sup> G. Lynch (private communication); Bull. Am. Phys. Soc. **10**, 133 (1966). We are indebted to Dr. Lynch for making available to us  $K^-p \rightarrow K^-p$  differential cross sections measured at 1.22, 1.43, 1.51, 1.61, 1.70, 1.80, 1.95, 2.08, 2.44, and 2.60 GeV/c  $K^-$  laboratory momenta and the result of his analysis.

<sup>7</sup> A. Fridman, O. Benary, A. Michalon, B. Schiby, R. Strub, and G. Zech, Phys. Rev. **145**, 1136 (1966).

<sup>8</sup> A. Fridman and A. Michalon, Nuovo Cimento **48A**, 344 (1967).

<sup>9</sup> R. J. N. Phillips and W. Rarita, Phys. Rev. **139**, B1336 (1965).

<sup>10</sup> J. Mott, R. Ammar, R. Davis, W. Kropac, A. Cooper, M. Derrick, T. Fields, L. Hyman, J. Loken, F. Schweingruber, and J. Simpson, Phys. Letters **23**, 171 (1966).

<sup>11</sup> Aachen-Berlin-CERN-London (I.C.)-Vienna Collaboration, Phys. Letters **24B**, 434 (1967).

<sup>12</sup> N. M. Gelfand, D. Harmsen, R. Levi Setti, M. Raymund, J. Doede, and W. Männer, Report No. 66-81 Enrico Fermi Institute for Nuclear Studies (EFINS) (unpublished).

<sup>13</sup> R. L. Cool, G. Giacomelli, T. F. Kycia, B. A. Leontić, K. K. Li, A. Lundby, and J. Teiger, Phys. Rev. Letters **16**, 1228 (1966). We are indebted to Dr. B. Leontić for kindly making available to us tabulated total-cross-section data.

<sup>14</sup> J. D. Davies, J. D. Dowell, P. M. Hattersley, R. J. Homer, A. W. O'Dell, A. A. Carter, K. F. Riley, R. J. Tapper, D. V. Bugg, R. S. Gilmore, K. M. Knight, D. C. Salter, G. H. Stafford, and E. J. N. Wilson, Phys. Rev. Letters **18**, 62 (1967).

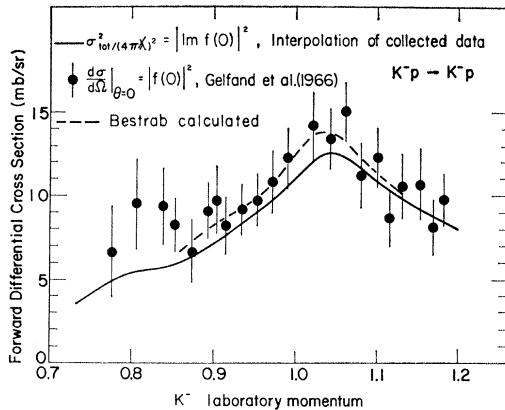


FIG. 2.  $K^-p \rightarrow K^-p$  forward differential cross sections. The experimental points, taken from Ref. 12, correspond to the extrapolation at  $0^\circ$  of sixth-order Legendre polynomial fits of Fig. 1. The full curve was obtained, using the optical theorem, from an interpolation of the total cross-section data of Refs. 13 and 14. The broken-line curve is the prediction of the model described here, for the best parameters obtained in a fit to the Legendre coefficients  $A_0$ - $A_5$  of Ref. 2.

in this comparatively low-energy domain, the scattering amplitude is already predominantly imaginary.

From the above evidence, it becomes plausible to attempt a parametrization of the background amplitudes, which accompany the resonant amplitudes in this region, in a form appropriate to describe diffraction scattering. With this in mind, we have fitted at small angles and  $P_{K^-} > 0.8$  GeV/c the angular distributions in

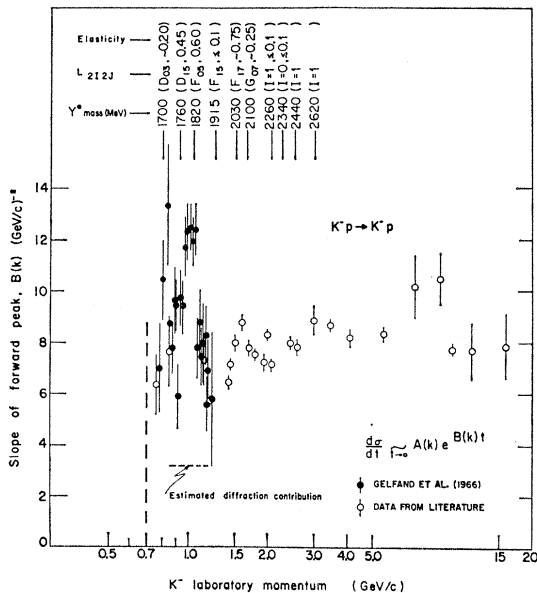


FIG. 3. Behavior of the slope  $B(k)$  of the forward peak in  $K^-p \rightarrow K^-p$  as a function of incident  $K^-$  momentum, obtained from fits of the differential cross sections to the form  $(d\sigma/dt) \sim A(k)e^{B(k)t}$ , for  $0 \leq -t < 0.4$  (GeV/c) $^2$ . The data have been taken from Refs. 4-7, 10, 11, 15-17. In the region 0.87-1.13 GeV/c, the best estimate of the diffraction contribution to  $B(k)$  is indicated by a dashed line.

the literature<sup>4-7,10,11,15-17</sup> to a differential cross section of the form

$$\frac{d\sigma}{dt} \approx \frac{\pi}{k^2} \frac{d\sigma}{d\Omega} \approx A(k)e^{B(k)t}. \quad (2)$$

The fits were obtained over those intervals of  $t$  which gave an acceptable  $\chi^2$ .

The behavior of  $B(k)$  as a function of  $K^-$  laboratory momentum is displayed in Fig. 3. Striking peaks are observed in this plot at  $K^-$  momenta corresponding to the formation of known resonances with large elasticity. Of particular prominence are the enhancements at  $\sim 800$  MeV/c, where the  $Y_0^*(1700)$  has been recently established,<sup>14,18</sup> and at  $\sim 1$  GeV/c, due to the combined effect of  $Y_1^*(1760)$  and  $Y_0^*(1820)$ . A similar effect is also noted at  $\sim 1.6$  GeV/c, a region where  $Y_1^*(2035)$  and  $Y_0^*(2100)$  are now known to exist,<sup>13,19</sup> and possibly at higher momenta. These effects correspond to an effective shrinking of the diffraction peak caused by the presence of high-spin resonances. This can be interpreted either in terms of an enhanced contribution of the high-resonating partial waves or, in optical language, as due to a widening of the absorptive disk.

It has been suggested by Damouth *et al.*,<sup>3</sup> for the analogous behavior in pion-proton elastic scattering, that the structure observed in  $B(k)$  could be effectively used as an experimental tool in the detection of resonant states.

Another feature of the behavior of  $B(k)$ , relevant to the parametrization of the diffractive background, is that  $B(k)$ , away from resonances, has practically a constant value of  $\sim (6-8)(\text{GeV}/c)^{-2}$ . This property, already observed at high momenta (see, e.g., Refs. 10 and 11), is now seen to hold throughout the explored range down to  $\sim 0.8$  GeV/c. Therefore, in constructing a diffractive-scattering amplitude (see Sec. 3) we will assume, in first approximation, an exponential form of constant slope.

In order to parametrize conveniently the diffractive contribution to  $A(k)$ , we have plotted in Fig. 4 the

<sup>15</sup> The points referred to Gelfand *et al.* (Ref. 12) in Fig. 3 were obtained from the data of Ref. 2 and from improved, unpublished data by the same authors.

<sup>16</sup> P. Bastien and J. P. Berge, Phys. Rev. Letters **10**, 188 (1963); W. Graziano and S. G. Wojcicki, Phys. Rev. **128**, 1868 (1962); M. N. Focacci, S. Focardi, G. Giacomelli, P. Serra, M. P. Zerbetto, and L. Monari, Phys. Letters **19**, 441 (1965).

<sup>17</sup> K. J. Foley, S. J. Lindenbaum, W. A. Love, S. Ozaki, J. J. Russell, and L. C. L. Yuan, Phys. Rev. Letters **11**, 503 (1963); K. J. Foley, R. S. Gilmore, S. J. Lindenbaum, W. A. Love, S. Ozaki, E. H. Willen, R. Yamada, and L. C. L. Yuan, *ibid.* **15**, 45 (1965).

<sup>18</sup> R. Armenteros, M. Ferro-Luzzi, D. W. G. Leith, R. Levi Setti, A. Minten, R. D. Tripp, H. Filthuth, V. Hepp, E. Kluge, H. Schneider, R. Barloutaud, P. Granet, J. Meyer, and J. P. Porte, in *Proceedings of the Thirteenth International Conference on Physics, Berkeley, California, 1966* (University of California Press, Berkeley, California, 1967).

<sup>19</sup> C. G. Wohl, F. T. Solmitz, and M. L. Stevenson, Phys. Rev. Letters **17**, 107 (1966).

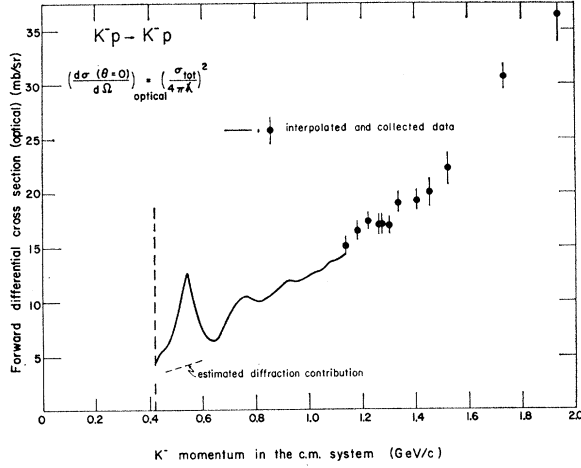


FIG. 4. Behavior of the optical point  $(d\sigma/d\Omega)_{\text{opt}} = (\sigma_{\text{tot}}/4\pi\lambda)^2$  as obtained from an interpolation of  $K^-p$  total-cross-section data of Refs. 13 and 14 (full line) and from the data of Refs. 4 and 20. In the region of  $K^-$  c.m. momenta 0.47–0.58 GeV/c, an estimate of the diffraction contribution is indicated by a dashed line.

behavior of the optical point

$$(d\sigma/d\Omega)_{\text{opt}} = (k/4\pi)^2 \sigma_{\text{tot}}^2 \quad (3)$$

as a function of the c.m.  $K^-$  momentum  $k$  as obtained from a collection of total-cross-section data.<sup>4,13,14,20</sup> The structure seen is the same structure present in the total cross section. Aside from the resonant bumps, a regular behavior is, however, apparent. This can be approximated, for  $k \lesssim 1$  GeV/c, by a linear functional dependence of  $(d\sigma/d\Omega)_{\text{opt}}$  versus  $k$ . At higher  $k$  values, however, as  $\sigma_{\text{tot}} \rightarrow \text{constant}$ ,  $(d\sigma/d\Omega)_{\text{opt}}$  increases quadratically with  $k$ . This information provides the parametrization sought.

A preliminary analysis along these lines for  $\pi^\pm p \rightarrow \pi^\pm p$  scattering has revealed features of these processes which are remarkably similar to those encountered above in  $K^-p \rightarrow K^-p$ . Thus, the slope  $B(k)$  becomes steeper in the vicinity of the high-spin  $N^*$  states of higher elasticity such as  $\Delta(1924)$ ,  $\Delta(2420)$ , etc. (see, e.g., Damouth *et al.*<sup>3</sup>).

Further detailed investigation is needed, in particular, for pion-nucleon and  $K^+$ -nucleon scattering, before the correct parametrization of the diffraction background for these processes may be given. In the Sec. 3 we will discuss, however, the problem of combining in a consistent fashion diffractive and resonant amplitudes for the general case of meson-nucleon scattering, and we will limit ourselves here to the case of  $K^-p \rightarrow K^-p$  as an application of the model.

### 3. DIFFRACTION AND RESONANT SCATTERING IN $(\pi, K)$ NUCLEON TWO-BODY PROCESSES

The scattering process, in a given isospin state, is described in terms of the scattering-amplitude matrix

$$M_I(k, \theta) = g_I(k, \theta) + ih_I(k, \theta) \sigma \cdot \hat{n}, \quad (4)$$

where  $k$  and  $\theta$  are the c.m. scattering variables.

For any specific  $\pi-N$  or  $K-N$  two-body process, the physical scattering amplitude is given by

$$M(k, \theta) = \sum_I C_I M_I(k, \theta) = g(k, \theta) + ih(k, \theta) \sigma \cdot \hat{n}, \quad (5)$$

where  $C_I$  are the appropriate isospin Clebsch-Gordan coefficients and  $g$ ,  $h$  are, respectively, the spin-nonflip and spin-flip amplitudes.

From Eq. (5) the differential cross section for an unpolarized target is

$$\frac{d\sigma}{d\Omega} = \frac{1}{2} \text{Tr}(MM^+) = |g(k, \theta)|^2 + |h(k, \theta)|^2, \quad (6)$$

and the polarization  $P(k, \theta)$  of the recoil nucleon is defined by

$$\frac{d\sigma}{d\Omega} P(k, \theta) = \frac{1}{2} \text{Tr}(MM^+ \sigma_n) = 2 \text{Im}[g(k, \theta)h^*(k, \theta)]. \quad (7)$$

The partial-wave decomposition of Eq. (4) yields

$$g_I(k, \theta) = \frac{1}{k} \sum_{l=0}^{\infty} [(l+1)a_{I,l+} + la_{I,l-}] P_l(x), \quad (8)$$

$$h_I(k, \theta) = \frac{1}{k} \sum_{l=1}^{\infty} [a_{I,l+} - a_{I,l-}] P_l^1(x),$$

$$= -\frac{1}{k} \sum_{l=1}^{\infty} [a_{I,l+} - a_{I,l-}] (1-x^2)^{1/2} \frac{dP_l(x)}{dx}, \quad (9)$$

where  $x = \cos\theta$ .

The physical partial-wave amplitudes  $A_{I\pm}$  are obtained from Eq. (5) as

$$A_{I\pm} = \sum_I C_I a_{I,l\pm} = \frac{1}{2i} (e^{2i\delta_{I\pm}} - 1). \quad (10)$$

We wish now to express the isospin amplitudes  $g_I(k, \theta)$  and  $h_I(k, \theta)$  in terms of diffractive and resonant contributions. For reasons of simplicity and in a pure phenomenological context, we have chosen to represent such amplitudes as a linear combination of diffractive and resonant terms which we shall denote by superscripts  $D$  and  $R$ , respectively:

$$g_I(k, \theta) = g_I^D(k, \theta) + g_I^R(k, \theta),$$

$$h_I(k, \theta) = h_I^D(k, \theta) + h_I^R(k, \theta). \quad (11)$$

Following the discussion in Sec. 2, we parametrize

<sup>20</sup> O. Chamberlain, K. M. Crowe, D. Keefe, L. T. Kerth, A. Lemonick, Tin Maung, and T. F. Zipf, Phys. Rev. **125**, 1696 (1962); W. F. Baker, R. L. Cool, E. W. Jenkins, T. F. Kycia, R. H. Phillips, and A. L. Read, *ibid.* **129**, 2285 (1963).

$g_I^D$  and  $h_I^D$  as<sup>21</sup>

$$\begin{aligned} g_I^D(k, \theta) &= G_I(k) \exp(b_I t), \\ h_I^D(k, \theta) &= H_I(k) (1-x^2)^{1/2} \exp(b_I' t), \end{aligned} \tag{12}$$

where  $b_I$  and  $b_I'$  are real constants,  $t = -2k^2(1-x)$ , and  $G_I(k)$ ,  $H_I(k)$  are complex functions.

The resonant contributions are given by

$$\begin{aligned} g_I^R &= \frac{1}{k} \sum_{l=l_R} [(l+1)a_{I, l_+^R} + l a_{I, l_-^R}] P_l(x), \\ h_I^R &= \frac{1}{k} \sum_{l=l_R} [a_{I, l_+^R} - a_{I, l_-^R}] (1-x^2)^{1/2} \frac{dP_l(x)}{dx}, \end{aligned} \tag{13}$$

where the sum extends over all resonant partial waves  $a_{I, l_{\pm}^R}$  with orbital angular momentum  $l_R$ . Such resonant partial waves can be parametrized by a suitable Breit-Wigner form.

The differential cross section, Eq. (6), and polarization, Eq. (7), are readily calculated from Eqs. (11)–(13) as functions of the diffraction and resonant parameters. For convenience these expressions are given in Appendix A.

Often, experimental scattering data are expressed in terms of Legendre series expansion for both differential

cross section and polarization;

$$\frac{d\sigma}{d\Omega} = \frac{1}{k^2} \sum_{n=0} A_n(k) P_n(x), \tag{14}$$

$$\frac{d\sigma}{d\Omega} P(k, \theta) = \frac{1}{k^2} \sum_{n=1} B_n(k) (1-x^2)^{1/2} \frac{dP_n(x)}{dx}. \tag{15}$$

Expressions for the  $A_n$  and  $B_n$  coefficients are derived by inverting Eqs. (14) and (15):

$$A_n(k) = \frac{k^2}{2} (2n+1) \int_{-1}^1 dx P_n(x) \frac{d\sigma}{d\Omega} \quad (n \geq 0), \tag{16}$$

$$\begin{aligned} B_n(k) &= \frac{k^2}{2} \frac{2n+1}{n(n+1)} \int_{-1}^1 dx (1-x^2)^{1/2} \\ &\quad \times \frac{dP_n(x)}{dx} \frac{d\sigma}{d\Omega} P(k, \theta) \quad (n \geq 1). \end{aligned} \tag{17}$$

The explicit expressions for  $A_n$ ,  $B_n$  in terms of the parameters of our model are obtained by inserting for  $d\sigma/d\Omega$  and  $P(k, \theta)$  in Eqs. (16) and (17) their expressions given in Eqs. (A1) and (A2). The results are as follows:

$$\begin{aligned} A_n(k) &= \frac{1}{2} k^2 (2n+1) \sum_{I, I'} C_I C_{I'} \{ \text{Re}[G_I G_{I'}^*] e^{-2k^2(b_I + b_{I'})} C_n[k^2(b_I + b_{I'})] + \text{Re}[H_I H_{I'}^*] e^{-2k^2(b_I' + b_{I}')} D_n[k^2(b_I' + b_{I}')] \} \\ &\quad + 2k(2n+1) \sum_I C_I e^{-2k^2 b_I} \sum_{l=l_R} \text{Re}\{ [(l+1)A_{l_+^R} + l A_{l_-^R}] G_I^* \} K_{ln}(2k^2 b_I) \\ &\quad + 2k(2n+1) \sum_I C_I e^{-2k^2 b_I'} \sum_{l=l_R} \text{Re}\{ [A_{l_+^R} - A_{l_-^R}] H_I^* \} H_{ln}(2k^2 b_I') \\ &\quad + (2n+1) \sum_{l=l_R} \sum_{l'=l_R} \text{Re}\{ [(l+1)A_{l_+^R} + l A_{l_-^R}] [(l'+1)A_{l_+^R} + l' A_{l_-^R}]^* \} I_{l'n} \\ &\quad + (2n+1) \sum_{l=l_R} \sum_{l'=l_R} \text{Re}\{ [A_{l_+^R} - A_{l_-^R}] [A_{l_+^R} - A_{l_-^R}]^* \} J_{l'n} \quad \text{for } n \geq 0, \end{aligned} \tag{18}$$

$$\begin{aligned} B_n(k) &= k^2 \frac{2n+1}{n(n+1)} \sum_{I, I'} C_I C_{I'} \text{Im}[G_I H_{I'}^*] e^{-2k^2(b_I + b_{I'})} E_n[k^2(b_I + b_{I'})] \\ &\quad + 2k \frac{2n+1}{n(n+1)} \sum_I C_I e^{-2k^2 b_I'} \sum_{l=l_R} \text{Im}\{ [(l+1)A_{l_+^R} + l A_{l_-^R}] H_I^* \} H_{nl}(2k^2 b_I') \\ &\quad + 2k \frac{2n+1}{n(n+1)} \sum_I C_I e^{-2k^2 b_I} \sum_{l=l_R} \text{Im}\{ [A_{l_+^R} - A_{l_-^R}]^* G_I \} N_{nl}(2k^2 b_I) \\ &\quad + 2 \frac{2n+1}{n(n+1)} \sum_{l=l_R} \sum_{l'=l_R} \text{Im}\{ [(l+1)A_{l_+^R} + l A_{l_-^R}] [A_{l_+^R} - A_{l_-^R}]^* \} J_{l'n} \quad \text{for } n \geq 1, \end{aligned} \tag{19}$$

where the functions  $C_n(y)$ ,  $D_n(y)$ ,  $F_n(y)$ ,  $K_{ln}(y)$ ,  $H_{ln}(y)$ ,  $N_{ln}(y)$ ,  $I_{l'n}$ , and  $J_{l'n}$  are defined in Eqs. (A3)–(A10).

<sup>21</sup> We have assumed that this parametrization for  $h_I^D$  is generally valid, although direct evidence is available to us only for  $\pi N$  scattering. See E. Predazzi and G. Soliani, Nuovo Cimento (to be published).

Furthermore, from Eqs. (11)–(13) we obtain for the partial-wave isospin amplitudes the expressions

$$\begin{aligned}
 a_{I,l+} &= a_{I,l+}{}^R \delta_{ll} + \frac{1}{2}(\pi/b_I)^{1/2} I_{l+1/2}(2k^2 b_I) e^{-2k^2 b_I} G_I(k) \\
 &\quad + \frac{1}{2}(\pi/b'_I)^{1/2} [l/(2l+1)] [I_{l-1/2}(2k^2 b'_I) - I_{l+3/2}(2k^2 b'_I)] e^{-2k^2 b'_I} H_I(k), \\
 a_{I,l-} &= a_{I,l-}{}^R \delta_{ll} + \frac{1}{2}(\pi/b_I)^{1/2} I_{l+1/2}(2k^2 b_I) e^{-2k^2 b_I} G_I(k) \\
 &\quad - \frac{1}{2}(\pi/b'_I)^{1/2} [(l+1)/(2l+1)] [I_{l-1/2}(2k^2 b'_I) - I_{l+3/2}(2k^2 b'_I)] e^{-2k^2 b'_I} H_I(k), \quad (20)
 \end{aligned}$$

where  $I_\nu(z)$  is the modified Bessel function of the first kind (see Appendix A).

The above set of relations represent the mathematical formulation of our model. We should point out that the explicit momentum dependence of  $G_I(k)$  and  $H_I(k)$  has been so far left arbitrary. Their parametrization as a function of  $k$ , within the scope of the present work, can only be obtained from an analysis of the forward differential cross sections and polarizations, as exemplified in Sec. 2 for  $K^-p \rightarrow K^-p$ .

#### 4. $K^-p \rightarrow K^-p$ DIFFRACTION AND RESONANT SCATTERING IN THE GeV REGION

We have specialized our model to interpret the  $K^-p \rightarrow K^-p$  differential cross sections between 0.85 and 1.2 GeV/c of Gelfand *et al.*<sup>2</sup> In this region, at least two resonant states<sup>22</sup> are known to exist. The first [ $Y_1^*(1760)$ ] is a  $D_{5/2}$ ,  $I=1$  state corresponding in our notation to  $a_{1,2+}{}^R$ . The second [ $Y_0^*(1820)$ ] is an  $F_{5/2}$ ,  $I=0$  state corresponding to  $a_{0,3-}{}^R$ . These resonant amplitudes are parametrized in the form

$$a^R = \frac{1}{2}x/(\epsilon - i), \quad (21)$$

where  $x = \Gamma_e(k)/\Gamma(k)$  is the elasticity of the resonance and  $\epsilon = 2(E_R - E)/\Gamma(k)$ . The  $l$  and  $k$  dependence of the widths was taken into account.<sup>23</sup>

For this particular problem we have considerably simplified the treatment of Sec. 3 in dealing with the diffractive amplitudes. First of all, we have set equal to zero the spin-flip part  $h_I^D$ . This assumption is based solely on considerations of simplicity in a first approximation. Clearly, it will become necessary to retain this term, with a suitable parametrization, if polarization data in this region, when available, were to indicate the presence of diffractivelike phenomena. Secondly, since we will describe here only a fit to  $K^-p \rightarrow K^-p$  and not to  $K^-p \rightarrow \bar{K}^0 n$ , we have replaced<sup>24</sup> the sum of the two isospin diffraction amplitudes  $g_0^D$  and  $g_1^D$  by a single

term  $g^D$  parametrized according to the analysis of Sec. 2.

The over-all scattering amplitudes then become

$$g(k, \theta) = ik \frac{G_1 + iG_2}{(\pi k)^{1/2}} e^{b\theta} + \frac{3}{k} [a_{1,2+}{}^R P_2(x) + a_{0,3-}{}^R P_3(x)], \quad (22)$$

$$h(k, \theta) = \frac{1}{k} (1-x^2)^{1/2} \left[ a_{1,2+}{}^R \frac{dP_2(x)}{dx} - a_{0,3-}{}^R \frac{dP_3(x)}{dx} \right]. \quad (23)$$

In Eq. (22), the imaginary part  $G_1$  of the diffractive amplitude is expected to be much larger than the real part  $G_2$ .

The partial-wave amplitudes, obtained by inverting Eqs. (22) and (23), are

$$a_{I,l\pm} = a_{I,l\pm}{}^R \delta_{ll} + ik \frac{G_1 + iG_2}{(4bk)^{1/2}} e^{-2bk^2} I_{l+1/2}(2bk^2). \quad (24)$$

The explicit expressions for the Legendre polynomial coefficients  $A_n$  (see Sec. 3) are given in Appendix B. These expressions have been fitted to the data of Gelfand *et al.*,<sup>2</sup> as already reported there. We will, on the other hand, discuss this fit (called BESTRAB) in more detail in the present work.

The parameters left free were the mass  $M$ , width  $\Gamma$ , and elasticity  $x$  of the two resonances and three diffraction parameters  $G_1$ ,  $G_2$ , and  $b$ . This nine-parameter fit was extended to  $A_0$ ,  $A_1$ ,  $A_2$ ,  $A_3$ ,  $A_4$ , and  $A_5$  within the momentum interval 0.87–1.13 GeV/c, where most of the contribution of  $Y_1^*(1760)$  and  $Y_0^*(1820)$  is contained. Beyond these limits other resonant states should be taken into account<sup>18</sup>; consequently, it is believed that, in this first test of the model, it is appropriate to restrict our analysis to the simplest situation. This is particularly important for a precise first estimate of the diffractive parameters since their determination might be ambiguous when a large number of resonances is present.

The search for a minimum  $\chi^2$  was executed by the program MINFUN<sup>25</sup> operating in its minimizing mode. The best fit had a  $\chi^2$  of 55.9 for 90 data points and 80 degrees of freedom for the following parameters

<sup>22</sup> For the abundant literature on  $Y_1^*(1760)$  and  $Y_0^*(1820)$  we refer to A. H. Rosenfeld, A. Barbaro-Galtieri, W. J. Podolsky, L. R. Price, P. Soding, C. G. Wohl, M. Roos, and W. J. Willis, *Rev. Mod. Phys.* **39**, 1 (1967).

<sup>23</sup> J. M. Blatt and V. F. Weisskopf, *Theoretical Nuclear Physics* (John Wiley & Sons, Inc., New York, 1952).

<sup>24</sup> This corresponds to the assumption that either the radii of interaction in the two isospin channels are comparable or that one of the two is much greater than the other.

<sup>25</sup> Program written at the Lawrence Radiation Laboratory by W. E. Humphrey, Alvarez Group Memo No. P. 6, 1962 (unpublished).

(solution A):

$$\begin{aligned}
 M_2 &= 1758 \pm 11 \text{ MeV}, \\
 \Gamma_2 &= 113 \pm 25 \text{ MeV}, \\
 x_2 &= 0.46 \pm 0.05, \\
 M_3 &= 1811 \pm 4 \text{ MeV}, \\
 \Gamma_3 &= 73 \pm 10 \text{ MeV}, \\
 x_3 &= 0.67 \pm 0.08, \\
 G_1 &= 3.73 \pm 0.12 \text{ (mb)}^{3/4}, \\
 G_2 &= 0.89 \pm 0.39 \text{ (mb)}^{3/4}, \\
 2b &= 3.2 \pm 0.13 \text{ (GeV}/c)^{-2},
 \end{aligned}$$

where the indices 2 and 3 refer to the orbital angular momentum of the resonances.

A satisfactory fit with a minimum number of parameters could also be obtained by setting  $G_2=0$ , namely, with a pure imaginary diffractive amplitude. This eight-parameter fit gave a  $\chi^2$  of 57.7 for 90 data points and 81 degrees of freedom for the following values (solution B):

$$\begin{aligned}
 M_2 &= 1770 \pm 11 \text{ MeV}, \\
 \Gamma_2 &= 158 \pm 38 \text{ MeV}, \\
 x_2 &= 0.46 \pm 0.04, \\
 M_3 &= 1814 \pm 3 \text{ MeV}, \\
 \Gamma_3 &= 70.5 \pm 9 \text{ MeV}, \\
 x_3 &= 0.61 \pm 0.07, \\
 G_1 &= 3.81 \pm 0.14 \text{ (mb)}^{3/4}, \\
 2b &= 3.1 \pm 0.18 \text{ (GeV}/c)^{-2}.
 \end{aligned}$$

As can be seen from a comparison of the two sets of fitted parameters, the more general assumption of a diffractive amplitude containing both real and imaginary parts yields a fit which is only slightly better than that without the inclusion of a real part.

The  $A_n$  coefficients for both fits are shown in Fig. 5 in comparison with the experimental points of Ref. 2.

Using the best parameters of solution A, the differential cross sections have been calculated, and they are compared in Fig. 1 with the experimental data and their Legendre polynomial expansion. As can be seen, the calculated differential cross sections are generally in agreement with experiment except perhaps for the region below 0.85 GeV/c, where the data were not used in the fit of solutions A and B and where the  $Y_0^*(1700)$  is expected to contribute. This disagreement is, on the other hand, identical in physical content with the discrepancies between BESTRAB calculated and the observed  $A_n$  coefficients below 0.85 GeV/c (see Fig. 5).

Clearly, the differential cross sections could have been fitted by our model from the very start, without going through the Legendre expansion. On the other hand, the plots of the variation of the  $A_n$ 's with incident  $K^-$  momentum give a visual appreciation of the

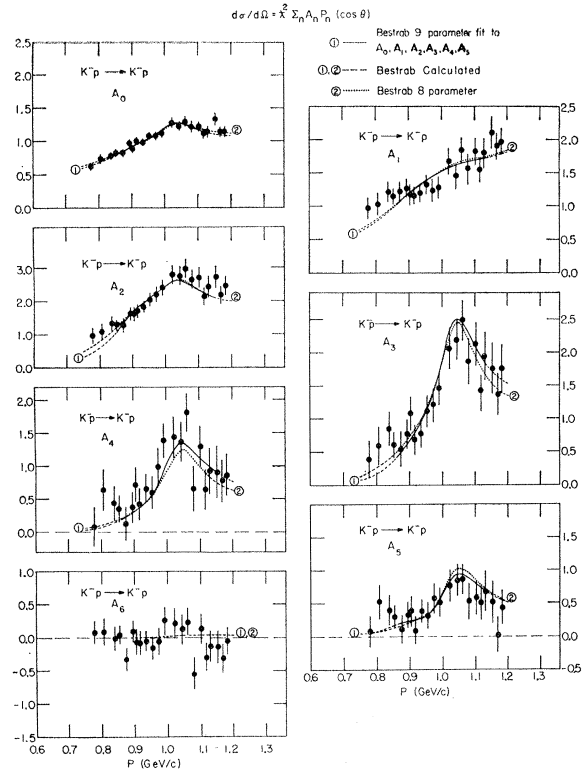


FIG. 5. Behavior of the Legendre polynomial coefficients  $A_n$  from a sixth-order expansion of the form  $d\sigma/d\Omega = \chi^2 \sum_n A_n P_n(\cos\theta)$ , as given by Gelfand *et al.* (Ref. 2) for  $K^-p \rightarrow K^-p$  from 0.777 to 1.183 GeV/c. The full line corresponds to the nine-parameter best fit to the data, using the model described in this paper (solution A, six resonant, three diffraction parameters). The dashed line corresponds to the eight-parameter best fit (solution B, six resonant and two diffraction parameters). In both cases the fit was limited to the region 0.87–1.13 GeV/c and included  $A_0$ – $A_5$ . Extrapolations from the fitted regions and the calculated behavior of  $A_6$  are also indicated.

resonant effects which would not be apparent in plots of  $d\sigma/d\Omega$ .

The calculated differential cross sections at  $0^\circ$  are also compared with the corresponding experimental points in Fig. 2 and are seen to interpolate satisfactorily the data in the region 0.87–1.13 GeV/c. The deviations of the experimental points from the behavior expected if the scattering amplitude were pure imaginary are now interpreted as being due mostly to the effects of the resonances in the region.

Finally, using Eq. (24) we have calculated the partial-wave amplitudes corresponding to solution A. These are shown in Fig. 6.

## 5. DISCUSSION AND CONCLUSIONS

As shown in Sec. 4, our approach of combining diffraction and resonant scattering has been highly successful in explaining  $K^-p \rightarrow K^-p$  scattering in the region of  $\sim 1$  GeV/c, where the large background amplitudes could be described by a minimal number of free parameters.

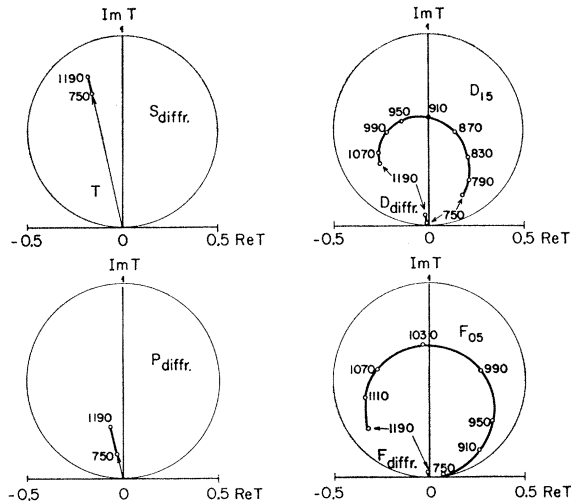


FIG. 6.  $K^-p \rightarrow K^-p$  partial-wave amplitudes as described by the model presented in this paper. The  $K^-$  laboratory momenta at which the amplitudes correspond are indicated for typical points.

The agreement of the  $Y_1^*(1760)$  and  $Y_0^*(1820)$  parameters with the values obtained in several other experiments has already been remarked upon by Gelfand *et al.*<sup>2</sup> In view of the large background present in this channel, a more detailed understanding of the situation concerning the formation of additional resonant states must await a considerable improvement of the statistical significance of the data. On the other hand, a new insight has been gained into the phenomena which accompany the formation of resonances and which must be taken into account for their study.

In particular, the implications of the above fit for what concerns the nonresonant  $K^-p \rightarrow K^-p$  interaction can be summarized as follows:

(a) The nature of the interaction is such as to meet the requirements for its description as diffraction scattering.

(b) The interaction is almost completely absorptive, since the ratio  $G_2/G_1$  is at most 20%, although not inconsistent with zero. This effectively corresponds to a "gray" (or "black") interaction region.

(c) The value of the forward differential cross section contributed by the imaginary part of the diffractive amplitude, indicated in Fig. 4 by a dashed line, is somewhat lower than could be anticipated from the behavior of  $(d\sigma/d\Omega)_{\text{opt}}$ , in the absence of resonant enhancements. Similarly, the slope  $2b = 3.2$  (GeV/c)<sup>-2</sup>, obtained for the diffractive part of the forward elastic peak, is lower than the asymptotic value of  $B(k)$  in Fig. 3. These discrepancies, and in particular the large variations between  $2b$  and  $B(k)$  which ranges from  $\sim 5.1$  to  $\sim 13$  (GeV/c)<sup>-2</sup>, are interpreted here as due to the resonant contributions and their interferences with diffraction. In effect, as previously pointed out, these

variations in  $B(k)$  constitute a sensitive signal of resonance formation.

(d) The relative magnitude and phase of all background partial waves is predicted by Eq. (24). They are slowly varying functions of  $k$  and decrease very rapidly with increasing  $l$ . The behavior of  $S_{\text{dif}}$ ,  $P_{\text{dif}}$ ,  $D_{\text{dif}}$ ,  $F_{\text{dif}}$  (see Fig. 6) is not inconsistent with an average over isospin and spin of the corresponding amplitudes obtained in a phase-shift analysis of  $K^-p \rightarrow \bar{K}^0 n$  data,<sup>18</sup> jointly with the  $K^-p \rightarrow K^-p$  data examined here and  $K^-p$  total cross sections.

We should remark at this point that our model has been so far tested in a very limited context only.

Possible isospin and spin dependences of the diffractive amplitudes could not be tested in  $K^-p \rightarrow K^-p$  scattering, which is already completely described by the simplified version of the model used in Sec. 4. Simultaneous fits to both  $K^-p \rightarrow K^-p$  and  $K^-p \rightarrow \bar{K}^0 n$  are presently in progress using the generalized model in order to separate the isospin contributions and will be described in a separate paper. More sensitive tests of the presence of a spin-flip term in the diffractive amplitude must, however, await the availability of polarization data in the same momentum region.

Clearly, a wide range of possible applications of the model exists; first in  $K^-p$  scattering, where our fit should be extended to cover a wider momentum region than considered here and where the effects of several additional resonant states might be detectable. A very promising region in this respect is that around 1.6 GeV/c, where considerable shrinking of the diffraction peak has been pointed out (see Fig. 3). Most of all, however, it will be crucial to attempt with our model to interpret  $\pi^\pm p$  elastic and charge-exchange scattering in the resonant region where much detailed information is available.

In extending our fit to a wider range of phenomena, it is appropriate to anticipate possible limitations which stem from the crudity of several of the assumptions made.

If indeed the background amplitudes, described here in terms of diffraction scattering, should be dominated by a Regge-type behavior, our parametrization  $g_l^D = G_l(k) \exp(b_l t)$  will have to be modified to include the proper logarithmic  $s$  dependence of the slope  $b_l$ . Over a small range of  $s$ , as in the application described here, and for  $t \rightarrow 0$ , however, the two behaviors coincide.

It is further to be remarked that the  $\exp(b_l t)$  dependence of  $g_l^D$  is, strictly speaking, only valid for small  $t$  values, since this behavior would lead to a violation of general requirements, such as analyticity and boundedness, when continued to large values of  $t$ .<sup>26</sup>

Another assumption which is quite arbitrary in our model is that of a linear decomposition of the amplitudes

<sup>26</sup> F. Cerulus and A. Martin, Phys. Letters 8, 80 (1964).



according to Eq. (11). There is at present no basis to justify this approach except in the fact that it leads to results which agree with experiment.

Finally, unitarity requirements are not explicitly imposed in the present version of our model. For the described application, the diffractive partial waves added very small contributions to the resonant  $D_{15}$  and  $F_{05}$  waves (see Fig. 6). Consequently, the violation of unitarity is quantitatively negligible, at least in this case. Had the resonances occurred in the lower partial waves, however, where the diffractive amplitudes are large, our parametrization could have been reinterpreted in terms of the  $K$ -matrix formalism. One could perhaps speculate that the observed diffraction effects themselves might be interpreted as a manifestation of

unitarity in the coherent-scattering process by a strongly absorptive region of interaction. If this were the case, and our formulation were sufficiently accurate, the experimental data would necessarily lead to a set of parameters satisfying the requirement of unitarity.

#### ACKNOWLEDGMENTS

We wish to thank Professor G. Wentzel for the most helpful criticism and suggestions and Professor R. H. Dalitz for illuminating discussions. We are indebted to Dr. N. M. Gelfand for much help and to B. Beeken for his valuable assistance in programming. One of us (R.L.S.) wishes to acknowledge the generous hospitality extended to him at CERN where this paper was written.

#### APPENDIX A

From Eqs. (4)–(7), (10)–(13) the explicit expressions for  $d\sigma/d\Omega$  and  $P(k, \theta) d\sigma/d\Omega$  within the generalized model of Sec. 3 are readily calculated, and one obtains

$$\begin{aligned} \frac{d\sigma}{d\Omega} &= \sum_{I, I'} C_I C_{I'} [\operatorname{Re}(G_I G_{I'}^*) e^{i(b_I + b_{I'})} + \operatorname{Re}(H_I H_{I'}^*) (1-x^2) e^{i(b'_{I'} + b'_{I'})}] \\ &+ \frac{2}{k} \sum_I C_I \sum_{l=l_R} \{ \operatorname{Re}[(l+1)A_{l+}^R + lA_{l-}^R] G_I^* \} e^{b_I l} P_l(x) + \operatorname{Re}[(A_{l+}^R - A_{l-}^R) H_I^*] (1-x^2) e^{b'_{I'} l} dP_l(x)/dx \\ &+ \frac{1}{k^2} \sum_{l=l_R} \sum_{l'=l_R} \operatorname{Re}\{ [(l+1)A_{l+}^R + lA_{l-}^R] [(l'+1)A_{l'+}^R + l'A_{l'-}^R]^* \} P_l(x) P_{l'}(x) \\ &+ \frac{1}{k^2} \sum_{l=l_R} \sum_{l'=l_R} \operatorname{Re}[(A_{l+}^R - A_{l-}^R)(A_{l'+}^R - A_{l'-}^R)^*] (1-x^2) \frac{dP_l(x)}{dx} \frac{dP_{l'}(x)}{dx}, \quad (\text{A1}) \end{aligned}$$

$$\begin{aligned} P(k, \theta) \frac{d\sigma}{d\Omega} &= 2 \sum_{I, I'} C_I C_{I'} [\operatorname{Im}(G_I H_{I'}^*)] (1-x^2)^{1/2} e^{i(b_I + b'_{I'})} \\ &+ \frac{2}{k} \sum_I C_I \sum_{l=l_R} \operatorname{Im}\{ [(l+1)A_{l+}^R + lA_{l-}^R] H_I^* \} (1-x^2)^{1/2} e^{i b'_{I'} l} P_l(x) \\ &+ \frac{2}{k} \sum_I C_I \sum_{l=l_R} \operatorname{Im}[(A_{l+}^R - A_{l-}^R)^* G_I] (1-x^2)^{1/2} e^{i b_I l} \frac{dP_l(x)}{dx} \\ &+ \frac{2}{k^2} \sum_{l=l_R} \sum_{l'=l_R} \operatorname{Im}\{ [(l+1)A_{l+}^R + lA_{l-}^R] (A_{l'+}^R - A_{l'-}^R)^* \} (1-x^2)^{1/2} P_l(x) \frac{dP_{l'}(x)}{dx}. \quad (\text{A2}) \end{aligned}$$

The above formulas, inserted in Eqs. (16) and (17), respectively, give rise to the explicit forms Eqs. (18) and (19) for the  $A_n$  and  $B_n$  coefficients of the Legendre series expansions Eqs. (14) and (15). In the following we give the definitions and the expressions of the functions  $C_n(y)$ ,  $D_n(y)$ ,  $\dots$ ,  $J_{l'n}$  by which the coefficients  $A_n$  and  $B_n$  in Eqs. (18) and (19) are expressed. For simplicity, we shall not give the details of the derivation of these functions, but simply state the results:

$$C_n(y) \equiv \int_{-1}^1 dx e^{2xy} P_n(x) = (\pi/y)^{1/2} I_{n+1/2}(2y), \quad (\text{A3})$$

$$D_n(y) \equiv \int_{-1}^1 dx e^{2xy} (1-x^2) P_n(x) = \frac{1}{y} \left( \frac{\pi}{y} \right)^{1/2} \left[ I_{n+3/2}(2y) - \frac{n^2-n}{4y} I_{n+1/2}(2y) \right], \quad (\text{A4})$$

$$E_n(y) \equiv \int_{-1}^1 dx e^{2xy} (1-x^2) \frac{dP_n(x)}{dx} = \left( \frac{\pi}{y} \right)^{1/2} \frac{n(n+1)}{2n+1} [I_{n-1/2}(2y) - I_{n+3/2}(2y)], \quad (\text{A5})$$

$$K_{ln}(y) \equiv \frac{1}{2} \int_{-1}^1 dx e^{xy} P_l(x) P_n(x) = \left(\frac{\pi}{2y}\right)^{1/2} \sum_{m=0}^{l+n} (2m+1) I_{m+1/2}(y) I_{lmn}, \tag{A6}$$

$$H_{ln}(y) \equiv \frac{1}{2} \int_{-1}^1 dx e^{xy} (1-x^2) P_n(x) \frac{dP_l(x)}{dx} = \left(\frac{\pi}{2y}\right)^{1/2} \frac{l(l+1)}{2l+1} \left[ \sum_{m=0}^{n+l-1} (2m+1) I_{m+1/2}(y) I_{l-1,n,m} - \sum_{m=0}^{n+l+1} (2m+1) I_{m+1/2}(y) I_{l+1,n,m} \right], \tag{A7}$$

$$N_{ln}(y) \equiv \frac{1}{2} \int_{-1}^1 dx e^{xy} (1-x^2) \frac{dP_l(x)}{dx} \frac{dP_n(x)}{dx} = n(n+1) K_{ln}(y) - y H_{nl}(y), \tag{A8}$$

$$I_{ln} \equiv \frac{1}{2} \int_{-1}^1 dx P_l(x) P_{l'}(x) P_n(x) = \frac{\Gamma\left(\frac{l+l'+n}{2}+1\right) \Gamma\left(\frac{l+l'-n+1}{2}\right) \Gamma\left(\frac{l+n-l'+1}{2}\right) \Gamma\left(\frac{l'+n-l+1}{2}\right)}{2\pi \Gamma\left(\frac{l+l'+n}{2}+\frac{3}{2}\right) \Gamma\left(\frac{l'+l-n}{2}+1\right) \Gamma\left(\frac{l+n-l'}{2}+1\right) \Gamma\left(\frac{l'+n-l}{2}+1\right)}, \tag{A9}$$

if  $l+l'+n = \text{even}$  and  $|l-l'| \leq n \leq l+l'$ ,  
 = 0 otherwise.

$$J_{ln} \equiv \frac{1}{2} \int_{-1}^1 dx (1-x^2) P_n(x) \frac{dP_l(x)}{dx} \frac{dP_{l'}(x)}{dx} = \frac{l(l+1)}{2l+1} \sum_{m=0}^{[(l'-1)/2]} (2l'-4m-1) [I_{l-1, l'-2m-1, n} - I_{l+1, l'-2m-1, n}], \tag{A10}$$

if  $l, l' \geq 1, l+l'+n = \text{even}$  and where  $0 \leq m \leq \text{maximum integer contained in } \frac{1}{2}(l'-1)$ ,  
 = 0 otherwise.

In Eqs. (A3)–(A8),  $I_\nu(y)$  is the modified Bessel function of the first kind,<sup>27</sup>

$$I_\nu(y) = \sum_{m=0}^{\infty} \frac{(y/2)^{2m+\nu}}{m! \Gamma(m+\nu+1)}. \tag{A11}$$

The integrals (A9) and (A10) are particular examples of Gaunt's integral,<sup>28</sup> which has been put into a form convenient for computational purposes.

**APPENDIX B**

The explicit expressions for the Legendre polynomial coefficients  $A_n$  relative to the simplified model used in Sec. 4 are obtained by the same techniques leading to Eqs. (18) and (19). In this particular case we get

$$A_n(k) = \frac{2n+1}{2(\pi 2b)^{1/2}} k^2 (G_1^2 + G_2^2) e^{-4bk^2} I_{n+1/2}(4bk^2) + B_n R + \frac{3}{4} (2n+1) \left(\frac{k}{b}\right)^{1/2} e^{-2bk^2} \frac{x_2}{\epsilon_2^2 + 1} (G_1 - G_2 \epsilon_2) \\ \times \left\{ I_{n+1/2}(2bk^2) \left[ 2 + \frac{3}{(2bk^2)^2} (n+1)(n+2) \right] - \frac{3}{bk^2} I_{n-1/2}(2bk^2) \right\} + \frac{3}{4} (2n+1) \left(\frac{k}{b}\right)^{1/2} e^{-2bk^2} \frac{x_3}{\epsilon_3^2 + 1} (G_1 - G_2 \epsilon_3) \\ \times \left\{ I_{n-1/2}(2bk^2) \left[ 2 + \frac{5}{(2bk^2)^2} (n^2 + n + 6) \right] - \frac{1}{2bk^2} I_{n+1/2}(2bk^2) \left[ 2(n+6) + \frac{(n+1)(n+2)(n+3)}{(2bk^2)^2} \right] \right\}, \tag{B1}$$

<sup>27</sup> A. Erdelyi, W. Magnus, F. Oberhettinger, and F. G. Tricomi, in *Bateman Manuscript Project, Higher Transcendental Functions* (McGraw-Hill Book Company, Inc., New York, 1953), Vol. II.  
<sup>28</sup> J. A. Gaunt, *Phil. Trans. Roy. Soc. (London)* **228**, 151 (1929).

where

$$\begin{aligned} B_0^R &= \frac{3}{4}X; & B_2^R &= (6/7)X; & B_4^R &= (9/14)X, \\ B_1^R &= (9/70)Y; & B_3^R &= (4/5)Y; & B_5^R &= (25/7)Y. \end{aligned} \quad (B2)$$

with

$$\begin{aligned} X &= x_2^2/(\epsilon_2^2+1) + x_3^2/(\epsilon_3^2+1), \\ Y &= \frac{x_2x_3}{(\epsilon_2^2+1)(\epsilon_3^2+1)}(1 + \epsilon_2\epsilon_3). \end{aligned} \quad (B3)$$

In (B1) and (B3),  $x_2, \epsilon_2$  refer to the  $Y_1^*(1760)$  and  $x_3, \epsilon_3$  to the  $Y_0^*(1820)$ .

## Field Theory of Chiral Symmetry

LOWELL S. BROWN\*

*Physics Department, Yale University,† Hew Haven, Connecticut*

and

*Stanford Linear Accelerator Center, Stanford University, Stanford, California*

(Received 17 July 1967)

An infinite class of chiral-invariant pion-nucleon Lagrange functions is discussed. Each member of this class is shown to be equivalent, under canonical transformation, to the one in which the commutator of the axial current with the meson field is an isotopic spin scalar. If the chiral symmetry is broken in this special canonical frame in a manner that ensures the partial conservation of the axial current, then the theory is unique.

THE application of chiral  $SU(2) \otimes SU(2)$  current algebra techniques to processes involving the emission and absorption of a large number of soft pions can become very cumbersome. Recently, Weinberg<sup>1</sup> has pointed out that this computational complexity can be reduced by employing an effective Lagrangian<sup>2</sup> that is chiral symmetric save for a part that yields a partially conserved axial current. Since such an effective Lagrangian satisfies all the constraints imposed by current algebra, it may be used in lowest order to obtain the kinematical and isotopic spin structure of the current algebra results for the behavior of scattering or decay amplitudes when the four momenta of various emitted (or absorbed) pions vanish. Higher-order corrections cannot alter this structure; they can only produce renormalization of coupling constants. The correct values of the coupling constants can be inferred<sup>1</sup> from the general structure of the current algebra method.

Weinberg<sup>1</sup> obtained an appropriate effective Lagrangian by first performing a canonical transformation on the  $\sigma$  model<sup>3</sup> and then sending the mass of the un-

physical  $\sigma$  particle to infinity so that it is removed from the theory. It is the purpose of this note to investigate an infinite class of chiral-invariant pion-nucleon Lagrange functions of the type introduced by Gürsey.<sup>4</sup> This class is restricted only in so far as the canonical pion-field momentum is required to involve the first but no higher derivatives of the pion field, with no dependence on the nucleon field. We shall show that in the limit of perfect chiral symmetry<sup>5</sup> every member of this class is equivalent, under canonical transformation,<sup>6</sup> to the one in which the commutator of the axial charge with the pion field is an isotopic spin scalar, a commutation relation characteristic of the  $\sigma$  model. Thus, in this limit, the physical scattering amplitudes are uniquely defined, although their off-mass-shell values

<sup>4</sup> F. Gürsey, *Nuovo Cimento* **16**, 230 (1960); in *Proceedings of the Tenth Annual International Conference on High-Energy Physics at Rochester, 1960*, edited by E. C. G. Sudarshan, J. H. Tincot, and A. C. Melissinos (Interscience Publishers, Inc., New York, 1961), p. 572; *Ann. Phys. (N. Y.)* **12**, 91 (1961).

<sup>5</sup> It is perhaps worthwhile to observe that if the theory is taken to be of a fundamental kind, not simply an effective Lagrangian that is used in lowest order, then in the perfect-chiral-symmetry limit the nucleon state occurs as a degenerate mass doublet of opposite parities. The symmetry-breaking interaction will remove the mass degeneracy and could possibly extinguish one of the states. There are presently two ( $\frac{1}{2}^-$ ) candidates for a chiral partner to the nucleon:  $N(1520)$  and a less well established  $N(1700)$  [Rosenfeld *et al.*, *Rev. Mod. Phys.* **39**, 1 (1967)].

<sup>6</sup> The importance of canonical transformation was emphasized to me in conversation with W. A. Bardeen and B. W. Lee. They have independently obtained results similar to those of this paper. Their work will appear in *Canadian Summer Institute Lectures* (W. A. Benjamin, Inc., New York, to be published).

\* Supported in part by the National Science Foundation and the U. S. Atomic Energy Commission.

† Present address.

<sup>1</sup> S. Weinberg, *Phys. Rev. Letters* **18**, 188 (1967).

<sup>2</sup> The utility of an effective-Lagrangian method has also been advocated, without regard to current algebra, by J. Schwinger, *Phys. Letters* **24B**, 473 (1967). See also J. A. Cronin, *Phys. Rev.* **161**, 1483 (1967).

<sup>3</sup> J. Schwinger, *Ann. Phys. (N. Y.)* **2**, 407 (1957); M. Gell-Mann and M. Levy, *Nuovo Cimento* **16**, 705 (1960).